System Identification to Characterise Shoulder Joint Dynamics in Two Degrees of Freedom

Yahya Z. Yahya*, *Student Member, IEEE,* Thor F. Besier, Andrew J. Taberner, *Senior Member, IEEE,* and Bryan P. Ruddy, *Member, IEEE*

Abstract— In this study, we present a new design of a shoulder perturbation robot that can characterise the dynamics of the shoulder in two degrees of freedom. It uses two linear electric motors to perturb the shoulder joint in internal/external rotation and abduction/adduction, and force and position sensors to measure the corresponding torque and angular displacement about the joint. System identification techniques are used to estimate the dynamics of the muscles around the joint. The advantage our apparatus offers over the existing ones is that it can efficiently transfer torque to the joint and measure its dynamics separately with minimal interference from soft tissues. We verified that the apparatus can accurately estimate joint dynamics by conducting tests on a phantom of known properties. In addition, experiments were conducted on a human participant. It has been demonstrated that the measured dynamics of participant's arm are repeatable. The potential impact of our apparatus is to be used in clinic as a diagnostic tool for rotator cuff injuries.

I. INTRODUCTION

Rotator cuff injury is the most common cause of shoulder related pain and disability [1]: It accounts for 4.5 million clinician visits and 250,000 surgeries in the United States every year with management cost of over four billion dollars per year [2]. A range of clinical tests are used to diagnose rotator cuff injuries. There are three main types of physical examinations; strength testing using dynamometry, isolated muscle strength testing, and laxity/stability testing [3]. Although some information about rotator cuff muscles, such as their strength in specific positions, can be obtained by these tests, clinical tests of rotator cuff injuries are unreliable and ineffective for precise diagnosis and rely upon clinicians' experience and intuition. In addition, CT and MRI imaging techniques, which are relatively expensive, might be required to confirm the diagnosis.

One alternative for diagnosing rotator cuff injuries is to use system identification techniques to quantify the function of the shoulder joint. System identification is defined as the process of estimating the mathematical model that describes a particular system when both the input and the output are known; it has often been used to characterise the dynamics of human joints [4]–[6].

In particular, endpoint stiffness robots have been used in previous studies to estimate the stiffness of the upper limb [7][8]. Such a robot measures the torque and position applied at the hand in two or three degrees of freedom (DOF) to study the potential changes in joint properties due to neuromuscular diseases [9], and to understand the neuromuscular control system of human joints [8]. However, due to the complexity of the neuro-musculoskeletal system of the human upper limb, the endpoint is insufficient to characterise the dynamics of the shoulder separately from other joints in the required DOF, and is associated with significant measurement errors [10][11]. These errors will ultimately lead to errors in the estimation of limb dynamics.

We present the design and implementation of an apparatus to characterise the dynamics of the shoulder joint. The contraction of rotator cuff muscles generates movement to the glenohumeral joint in internal/external rotation (subscapularis, infraspinatus and teres minor) or in abduction/adduction (supraspinatus). Our apparatus was designed to perturb the glenohumeral joint in these DOF, which are relevant to the function of the rotator cuff muscles. The device can accurately measure the applied torque and its corresponding angular position about the joint in each DOF. The advantage of our apparatus over previous designs is that it can efficiently transfer the required torque to the shoulder separately from other joints with minimal interference from other soft tissues within the upper limb. We use parametric and non-parametric system identification algorithms to analyse the experimental torque and position data and to estimate the system parameters representing the shoulder. Initial results demonstrate the feasibility of the apparatus using real data collected from one human participant.

II. METHODS

A. Experimental Apparatus Design

The apparatus (perturbation robot) was designed to generate a small perturbation to the rotator cuff muscles in the directions they are acting. Therefore, we designed our apparatus to perturb the shoulder joint in these DOF. Unfortunately, the glenohumeral joint cannot be perturbed proximally as the humerus is surrounded by muscles and other soft tissues, and therefore the torque should be applied distally to the forearm.

The perturbation robot consists of a forearm exoskeleton, two voice coil linear actuators, force and position sensors, and bearings (Fig. 1). Parts were assembled to an aluminium plate. The exoskeleton can be easily attached to the participant's forearm and adjusted for different sizes. It has straps and two C-clamps to firmly attach the bony aspects of the forearm at the wrist and epicondyles. This attachment reduces interference from soft tissues and ensures efficient transfer of torque to the rotator cuff muscles. The exoskeleton of the perturbation robot is actuated by two voice coil linear actuators (BEI Kimco, LA-25-42-000A) of ± 86.3 N continuous stall force and 25.4 mm total stroke. These actuators are controlled to generate perturbations in internal/external rotation and abduction/adduction, up to ± 20 N.m torque and ± 3.6° angular displacement. The apparatus is equipped with two tension/compression force sensors (HBM, U9C ±100N) and two linear potentiometers (Alps Alpine, RDC10320RB) to measure the perturbation torque and angle, respectively. This design enables multiple degrees of freedom to be explored in different configurations.
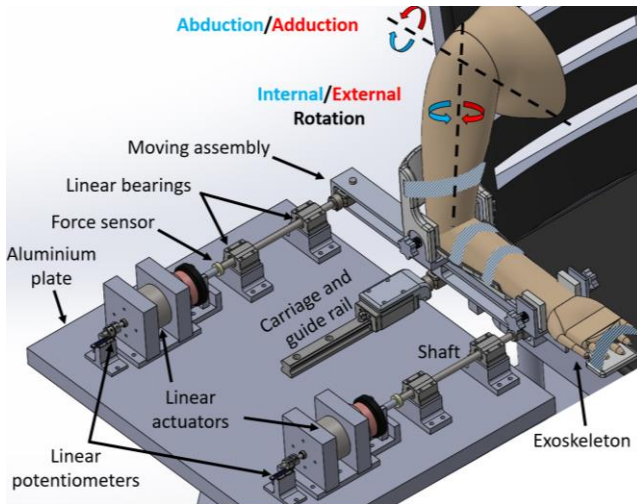

Figure 1. A CAD model showing the designed experimental apparatus (perturbation robot) used to generate two DOF perturbation and to measure the torque and angular displacement about the glenohumeral (shoulder) joint.

Switching between the two DOF is obtained by changing the polarity of one of the linear actuators. Abduction/adduction can be achieved by synchronising the movement of the two actuators so that they travel the same distance in the same direction. Internal/external rotation is achieved if the two linear actuators travel the same distance but in opposite directions.

The robot can create motion in internal/external rotation without inducing any bending forces. This was achieved by having clevis joints (at the two sides of the moving assembly) which allow small movement in the in the perpendicular direction to compensate for distance change with respect to centre of rotation. In internal/external rotation, the linear stage and the centre of rotation will not move. In abduction/adduction, the required angle is very small and therefore exoskeleton motion can be linear.

The required perturbation DOF, amplitudes and frequency bands are achieved by controlling the position of both linear actuators using a National Instruments c-RIO-9056 real-time

controller. It is equipped with motor drive modules (NI 9505) to drive the linear actuators, and analogue input modules (NI 9237 and NI 9215) to acquire data from the force and position sensors respectively. LabVIEW was used to monitor and control the system. Following each experiment, data analysis was performed using MATLAB.

B. Experimental Procedure

The perturbation robot was first tested on an upper limb phantom (Fig. 2) of known inertial, and stiffness parameters for verification (I=0.0818 kg.m², K=7.20 N.m/rad in internal/external rotation, and I=0.434 kg.m², K=16.20 N.m/rad in abduction/adduction). This phantom has been designed and implemented to mimic the dynamics of the shoulder with a simple spring-mass-damper system in both internal/external rotation and abduction/adduction (due to the role of stabilising soft tissue structures in these rotational DOF). Linear springs were used to create angular stiffness in those two DOF as the angular displacement is relatively small Perturbation experiments were also performed on one human participant; the experimental procedure was approved by The University of Auckland Human Participants Ethics Committee (protocol 024075).
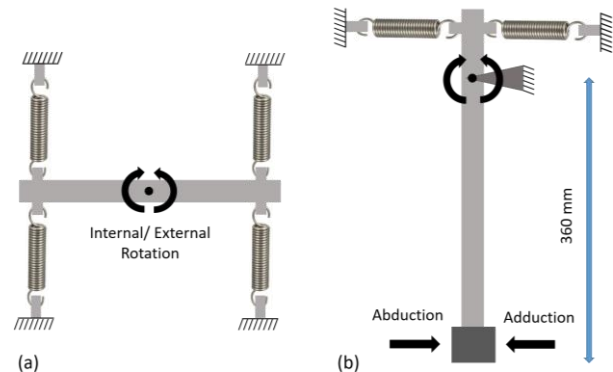

Figure 2. A schematic diagram of the two DOF phantom having inertial, viscous and stiffness components: (a) top view (b) front view.

The participant was seated on a height adjustable chair next to the robot with their arm in neutral rotation and their forearm and hand at 90° flexion to point forward (with palm up). The exoskeleton of the robot was then attached to the forearm and the hand of the participant at this position. This robot has adjustable wrist and elbow grabs and straps to minimise any possible movement. There might be some laxity at elbow joint when perturbation torque is applied. However, flexed elbow position (90°) minimises laxity and maximises elbow stiffness, making it much higher than shoulder stiffness and therefore elbow laxity is insignificant. In the last step, the participant's torso was strapped to the back of the chair to minimise torso movement during perturbation.

Next, angle controlled white noise perturbation signals in a frequency band from 0.1 Hz to 25 Hz with maximum amplitudes of 0.04 rad were applied by the exoskeleton. White noise was chosen as it can excite the shoulder at all intended frequencies with equal intensities, to fully investigate system behavior which might be more complicated than second order spring-mass-damper. The perturbations were performed in two modes: abduction/adduction and internal/external rotation. For each

mode, the experiment was repeated five times while the arm was fully relaxed and five times while the arm was voluntarily contracted. The perturbation in each trial took about 10 seconds. The participant was offered few minutes of rest break after each perturbation to avoid fatigue.

The measured torque and angular position data were evaluated using two approaches: a **non-parametric** approach to represent the dynamics by a compliance frequency response function (FRF) [12], and a **parametric** approach using the extended Kalman filter (EKF) algorithm [13] which can estimate the system's unknown parameters. For the parametric approach, the system was represented by a linear second order model with inertial (I), viscous (B) and stiffness (K) parameters.

III. Results

A. Non-parametric Approach

Non-parametric compliance FRFs and their associated coherence functions in internal/external rotation and abduction/adduction are shown in Fig. 3. Results from four cases are presented: robot only, with phantom, with relaxed arm and with contracted arm. In the last three cases, the dynamics of the perturbation robot are integrated into those of the phantom or the arm.
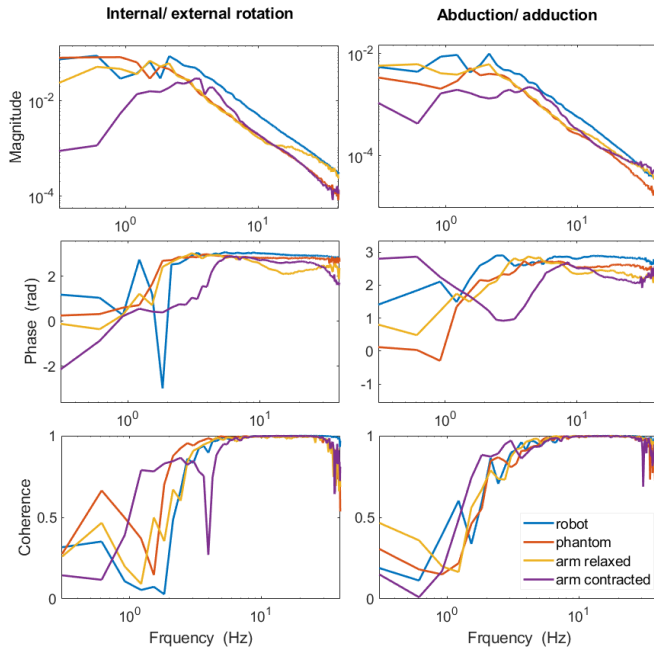
Figure 3. Measured compliance FRF and coherence by the perturbation robot in four cases (robot only, with phantom, with arm relaxed and with arm contracted) in internal/external rotation and abduction/adduction.

B. Parametric Approach

Inertial (I), viscous (B) and stiffness (K) parameters for all trials were estimated using the EKF algorithm. Fig. 4 shows parameter convergence of the subject's arm dynamics over time in abduction/adduction in two cases: relaxed arm and contracted arm. For each case results from five trials are presented. These parameters represent the arm's parameters plus the perturbation robot's parameters.

Tables I and II show the estimated parameters of the perturbation robot, the phantom and the arm. In addition, they compare the theoretically calculated and estimated parameters for the perturbation robot and the phantom. However, there was not enough information to calculate predicted viscous parameters and therefore they were left blank in the tables. The robot's parameters were subtracted from those of all other cases to isolate the dynamics of the system being measured.
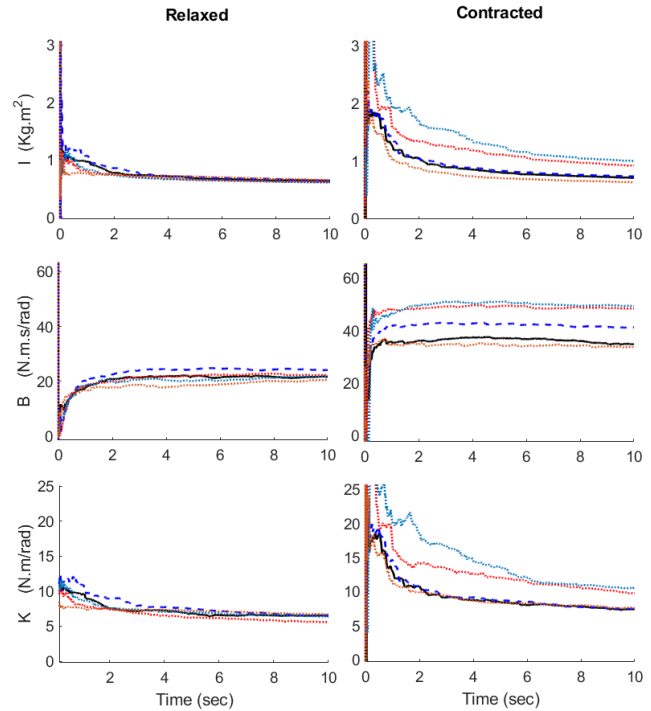
Figure 4. Extended Kalman filter (EKF) estimates of abduction/adduction I, B and K parameters, of the robot and the arm together, in two cases (arm relaxed and contracted). In each case, data were collected from five separate trials.

TABLE I.   PARAMETER ESTIMATES IN INTERNAL/EXTERNAL ROTATION

I/E rotation Parameters	I (kg.m^2)	B (N.m.s/rad)	K (N.m/rad)
Robot (theor.)	0.0500	---------	0.00
Robot (meas.)	0.0497	0.47	0.55
Phantom (theor.)	0.0818	---------	7.20
Phantom (meas.)	0.0813	0.45	7.45
Arm relaxed (Average ± SD)	0.0483±0.0082	3.03±0.350	0.52±0.148
Arm contracted (Average ± SD)	0.0650±0.0160	3.13±0.526	2.71±0.487

TABLE II.   PARAMETER ESTIMATES IN ABDUCTION/ADDUCTION

Ab/Adduction Parameters	I (kg.m^2)	B (N.m.s/rad)	K (N.m/rad)
Robot (theor.)	0.400	---------	0.00
Robot (meas.)	0.422	5.10	4.01
Phantom (theor.)	0.434	---------	16.20
Phantom (meas.)	0.412	7.93	15.35

Arm relaxed (Average ± SD)	0.310±0.024	17.11±1.480	2.47±0.441
Arm contracted (Average ± SD)	0.330±0.152	35.70±5.540	5.02±1.414

IV. Discussion

The results show that the measured parameters closely matched the theoretically predicted ones. However, there was a difference of 4 N.m/rad in the stiffness estimate for the robot in ab/adduction. This difference was most likely caused by fitting a model of I, B and K to data from a robot that has only inertial and viscous dynamics ($K = 0$ N.m/rad).

The data from the human participant illustrates a distinct increase in the stiffness parameter, K, with muscle contraction. That implies that when the rotator cuff muscles contract to resist the perturbation, they stiffen the joint and maintain the arm in its reference position. The viscous parameter, B, also increased in the case of ab/adduction. In general, the arm offers a low stiffness compared to its mass and viscous damping.

These measurements from the same participant were repeatable when the arm was fully relaxed, supporting the exploration of comparative studies within and between individuals. Less repeatability was achieved when the participant voluntarily contracted their arm, which was likely due to inconsistency in contraction amount in the different trials. Fatigue might also influence dynamic contractions. In the future, EMG feedback might be used to improve the repeatability of the muscle contraction.

Fig. 4 shows that 2-3 seconds are required for the parameters in case of relaxed arm to converge to steady state. Longer time was required to achieve steady state for the contracted arm. The results also show that contracted arm parameters do not fully converge to constant values even after 10 seconds of EKF operation. This is likely due to muscle fatigue and contraction inconsistency which consequently lead to system non-linearity.

Non-parametric analysis showed the differences in compliance between the four cases in both DOF. In general, it can be said that the contracted arm has less compliance than the relaxed arm at low frequency. This is caused by increasing the stiffness and damping parameters which dominate the FRF. At high frequencies the compliance becomes the same, as the FRF in this case is dominated by the inertial effects. The observed coherence function suggests poor linearity and/or high noise at low frequencies, where the system is dominated by the stiffness and damping effects. Therefore, non-linear models would be better fitted to the measured data to give a better estimation of the parameters, especially at low frequencies.

V. Conclusion

This paper presented a new design of shoulder perturbation apparatus that can characterise the dynamics of rotator cuff muscles in two DOF. Verification from tests on a phantom with known dynamics showed that the robot accurately measured the dynamics of the shoulder. It has been also demonstrated that repeatable results can be achieved from multiple trials. That would prove the feasibility of using the device for detecting arms' dynamics differences between participants and track any changes in those dynamics which might occur due to injuries.

In the future, perturbation experiments will be conducted on a larger population of healthy participants to characterise the dynamics of their rotator cuff muscles, and to explore differences between dominant and non-dominant sides. Then, injured participants will be recruited to investigate any potential changes in their dynamics due to injuries. Nonlinear models and system identification techniques will also be explored, as they are more appropriate to represent real dynamics of muscle and tissue which are inherently nonlinear.

References

[1] R. S. Siegbert Tempelhof, Stefan Rupp, "Prevalence of Rotator Asymptomatic Shoulders," *J. shoulder Elb. Surg.*, vol. 8, no. 4, pp. 296–299, 1999.

[2] M. Petri, "Editorial: Current Treatment Options for Rotator Cuff Tears," *Open Orthop. J.*, vol. 10, no. 1, pp. 264–265, 2016.

[3] M. A. Ciccotti, M. C. Ciccotti, M. G. Ciccotti, A. J. Cosgarea, and P. P. Castle, "Rotator Cuff Injury," *Orthop. Sport. Med.*, vol. 2, pp. 1–12, 2005.

[4] J. H. Pasma, J. Van Kordelaar, D. De Kam, V. Weerdesteyn, A. C. Schouten, and H. Van Der Kooij, "Assessment of the underlying systems involved in standing balance: The additional value of electromyography in system identification and parameter estimation," *J. Neuroeng. Rehabil.*, vol. 14, no. 1, pp. 1–17, 2017.

[5] P. H. Chang, K. Park, S. H. Kang, H. I. Krebs, and N. Hogan, "Stochastic estimation of human arm impedance using robots with nonlinear frictions: An experimental validation," *IEEE/ASME Trans. Mechatronics*, vol. 18, no. 2, pp. 775–786, 2013.

[6] W. F. Genadry, R. E. Kearney, and I. W. Hunter, "Dynamic relationship between EMG and torque at the human ankle: Variation with contraction level and modulation," *Med. Biol. Eng. Comput.*, vol. 26, no. 5, pp. 489–496, 1988.

[7] J. J. Palazzolo, M. Ferraro, H. I. Krebs, S. Member, D. Lynch, and B. T. Volpe, "During Robotic Stroke Rehabilitation," vol. 15, no. 1, pp. 94–103, 2007.

[8] A. Ajoudani, C. Fang, N. Tsagarakis, and A. Bicchi, "Reduced-complexity representation of the human arm active endpoint stiffness for supervisory control of remote manipulation," *Int. J. Rob. Res.*, vol. 37, no. 1, pp. 155–167, 2018.

[9] J. J. Palazzolo, M. Ferraro, H. I. Krebs, S. Member, D. Lynch, and B. T. Volpe, "During Robotic Stroke Rehabilitation," *Rehabilitation*, vol. 15, no. 1, pp. 94–103, 2007.

[10] C. Fang, A. Ajoudani, A. Bicchi, and N. G. Tsagarakis, "Online Model Based Estimation of Complete Joint Stiffness of Human Arm," *IEEE Robot. Autom. Lett.*, vol. 3, no. 1, pp. 84–91, 2018.

[11] C. Wei, C. Y. Chen, X. Gao, G. Yang, G. Zhang, and Z. Fang, "Research on human upper limb endpoint mechanical impedance with multi-task environment," *Proc. 4th IEEE Int. Conf. Appl. Syst. Innov. 2018, ICASI 2018*, pp. 494–497, 2018.

[12] P. E. Wellstead, "Non-parametric methods of system identification," *Automatica*, vol. 17, no. 1, pp. 55–69, 1981.

[13] Y.-R. Kim, S.-K. Su, and M.-H. Park, "Speed Sensorless Vector Control of Filter," *IEEE Trans. Ind. Appl.*, vol. 30, no. 5, pp. 1225–1233, 1994.